ELSEVIER

Chemical Engineering Journal 134 (2007) 78–83

Chemical Engineering Journal

www.elsevier.com/locate/cej

Novel catalytic non-thermal plasma reactor for the abatement of VOCs

Ch. Subrahmanyam, A. Renken, L. Kiwi-Minsker*

Department of Chemical Engineering, GGRC-EPFL, 1015 Lausanne, Switzerland

Abstract

A novel dielectric barrier discharge (DBD) reactor has been designed and tested for the abatement of diluted volatile organic compounds (VOCs) of different nature. The novelty of the DBD reactor is that a metallic catalyst made of sintered metal fibers (SMF) also acts as the inner electrode. The SMF electrodes modified with oxides of Ti, Mn and Co were efficient during the destruction of toluene, isopropanol (IPA) and trichloroethylene (TCE). Total oxidation of IPA was achieved at lower specific input energy (SIE) compared to toluene and TCE. Among the catalysts studied, MnO_x/SMF showed the best performance, involving the formation of active oxygen species by *in situ* decomposition of ozone on the catalyst surface. The selectivity to CO_2 as the total oxidation product during TCE destruction was improved up to ~70% by modifying MnO_x/SMF with TiO_2.

Keywords: Non-thermal plasma; Dielectric barrier discharge; VOC abatement; Plasma photocatalysis; Sintered metal fibers

1. Introduction

The emission of volatile organic compounds (VOCs) by various industrial and automobile sources into the atmosphere is an important social concern as most of them are carcinogens and harmful to living organisms [1]. Abatement of air polluting substances are handled in three ways: electrostatic precipitators to collect the dusty particles, adsorption of gaseous pollutants by water scrubbers or adsorbent filters, and conversion of pollutants to harmless and/or useful products [1–3]. For the abatement of dilute VOCs (<1000 ppm), conventional techniques like adsorption, thermal, and thermocatalytic oxidation are not suitable, mainly due to high-energy consumption [4,5].

Among the alternatives, non-thermal plasma (NTP) generated at atmospheric pressure has been receiving increasing attention avoiding the heating during the treatment [5]. The specific advantage of NTP is selective production of energetic electrons without heating the flue gas [5–7]. In dielectric barrier discharge (DBD), the dielectric barrier distributes the microdischarges throughout the discharge volume initiating the chemical reactions by reactive species like ions, radicals and activated molecules [4–8]. The performance of the NTP reactor depends on the utilization of the short-lived species formed in plasma [5,9,10]. The efficiency of NTP reaction has been addressed based on reducing the power consumption and suppressing the undesired by-product formation. A variety of DBD reactors have been used for the destruction of various VOCs, however, the desired total oxidation to CO_2 and H_2O was not achieved [11–13]. In addition, formation of toxic by-products like CO, NO_x and O_3 was observed [14].

To overcome these limitations, catalytic plasma technique has been proposed, where the catalyst is placed either in the discharge zone (in-plasma catalytic reactor) or after the discharge zone (post-plasma catalytic reactor) [6,9–15]. In-plasma catalytic reactor was found to enhance the oxidation of VOCs. A synergy was due to short-lived plasma species and *in situ* formation of atomic oxygen by the decomposition of ozone. However, the main disadvantage is fast deactivation of the catalyst because of the carbonaceous deposit. Like-wise, performance of the plasma reactor increased when the catalyst was placed down stream to the discharge zone. This was attributed to the oxidizing properties of long-lived species, mainly ozone and oxides of nitrogen. However, short-lived oxidizing species cannot reach the catalyst surface in this configuration.

During the present study, a novel DBD reactor has been designed, where the catalyst made of sintered metal fiber (SMF) filter also acts as the inner electrode. The SMF electrode was modified with transition metal oxides. Abatement of selected VOCs of different nature like toluene, isopropanol (IPA) and trichloroethylene (TCE) was tested to evaluate the performance of the catalytic DBD reactor. Influence of applied voltage, frequency and the formation of ozone on the performance of this DBD reactor were also studied.

* Corresponding author. Tel.: +41 21 693 3182; fax: +41 21 693 3190.
E-mail address: lioubov.kiwi-minsker@epfl.ch (L. Kiwi-Minsker).

1385-8947/$ – see front matter © 2007 Elsevier B.V. All rights reserved.
doi:10.1016/j.cej.2007.03.063

2. Experimental

2.1. Materials and catalyst preparation

Sintered metal fibers filters (Southwest Screens & Filters SA, Belgium) made of stainless steel consists of thin uniform metal fibers (Ø40 μm) and has a wetness capacity of ~30 wt%. For the preparation of 3 wt% MnO_x and CoO_x on SMF, stainless steel filters were oxidized in flame, followed by impregnation with Co and Mn nitrate aqueous solutions of desired concentrations. TiO_x/SMF and TiO_x/MnO_x/SMF were prepared by precipitation of Ti-(IV) bis (ammonium lactato) dihydroxide, 50 wt% solution in water. Drying at room temperature followed by calcination in air at 773 K for 5 h results metal oxide supported SMF catalysts. Finally, SMF filters were subjected to an electrical hot press to get them in cylindrical form.

2.2. Experimental set-up and procedure

The experimental set-up consisted of a motor driven syringe pump for the introduction of VOC, which was mixed with air (500 ml (STP)/min for toluene, IPA and 700 ml (STP)/min for TCE) in a mixing chamber, which was electrically heated. The input concentration of VOC was fixed at 250 ppm and was fed into the plasma reactor with a Teflon tube. VOC concentration at the outlet was measured with a gas chromatograph (Shimadzu 14B) equipped with a FID and a SP-5 capillary column. The formation of CO_2 and CO was simultaneously monitored with an infrared gas analyzer (Siemens Ultramat 22), whereas, ozone formed in the plasma reactor was measured with an UV absorption ozone monitor (API-450 NEMA). As the volume change due to chemical reactions are negligible, selectivity of CO_2 and CO_x was defined as:

$$S_{CO_2}(\%) = \frac{[CO_2]}{X([VOC]_0 - [VOC])} \times 100$$

$$S_{CO_x}(\%) = \frac{[CO] + [CO_2]}{X([VOC]_0 - [VOC])} \times 100$$

where $X = 7$, 3 and 2 for Toluene, IPA and TCE, respectively.

2.3. Plasma reactor and power supply

A detailed description of the novel DBD reactor has been published elsewhere [16]. Briefly, the dielectric discharge was generated in a cylindrical quartz tube with an inner diameter of 19 mm. Silver paste painted on the outer surface of the quartz tube acts as the outer electrode, whereas, the SMF filter in the form of a cylindrical tube as the inner electrode. The discharge length was 10 cm and the discharge gap was fixed at 3.5 mm during the destruction of toluene and IPA, whereas, it was varied between 3.5 and 1.25 mm for TCE. One end of SMF filter was connected AC high voltage through a copper rod, whereas, the other end was connected to the inlet gas stream through a Teflon tube. The AC high voltage in the range 12.5–22.5 kV (p–p) was applied between the two electrodes and frequency was varied between 200 and 350 Hz. Conversion of VOC at each voltage was measured after 30 min. A *V–Q* Lissajous method was used to determine the discharge power (W) in the plasma reactor, where the charge *Q* (i.e. time integrated current) was recorded by measuring the voltage across the capacitor of 100 nF connected in series to the ground electrode. Applied high voltage was measured with a 1000:1 high voltage probe (Fluke 80 K-40 HV). The signals of *V* and *Q* were recorded with a digital oscilloscope (Tektronix, TDS 3054) and plotted to get a typical *V–Q* Lissajous diagram as shown in Fig. 1a.

3. Results

3.1. Discharge characterization

Fig. 1a represents a typical *V–Q* Lissajous figure at a constant frequency of 350 Hz for 3.5 mm discharge gap. The average power (W) dissipated in the discharge was calculated by multiplying the area of the Lissajous figure with the frequency and the capacitance. The specific input energy (SIE) was calculated

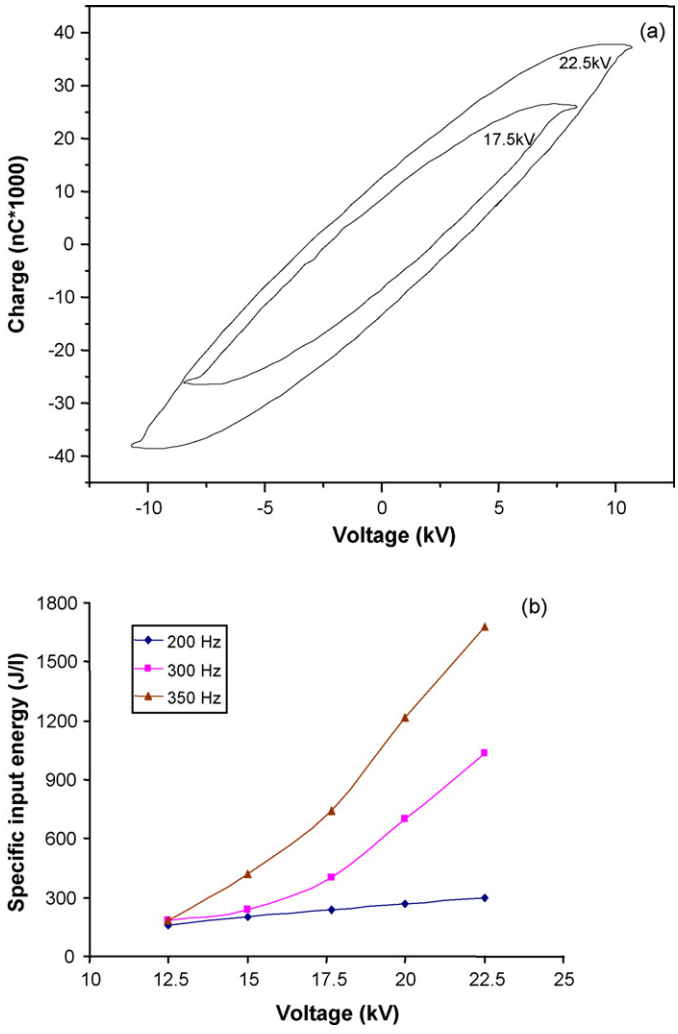

Fig. 1. (a) *V–Q* Lissajous figure at 350 Hz and (b) variation of SIE as a function of voltage and frequency for 3.5 mm discharge gap.

using the relation:

$$\text{Specific input energy (SIE) (J/l)} = \frac{\text{discharge power (W)}}{\text{gas flow rate (l/s)}}$$

Increasing the applied voltage at a constant frequency increases the power (Fig. 1a) and the specific input energy (Fig. 1b). For example, at 200 Hz, the SIE increased from 160 J/l (12.5 kV) to 295 J/l (22.5 kV). With increasing frequency to 300 and 350 Hz, at 22.5 kV, SIE increases to 1030 and 1650 J/l, respectively.

3.2. Catalytic non-thermal plasma reactor for destruction of toluene

Fig. 2 shows the activity of metal oxide supported SMF electrodes during the destruction of 250 ppm of toluene at a SIE 160 J/l (12.5 kV and 200 Hz). Non-modified SMF showed conversion of ~60%, which increased to ~70% with CoO_x and MnO_x/SMF. Important is that metal oxide supported SMF electrodes showed higher CO_x selectivity. >55% selectivity to CO_x was observed for CoO_x and MnO_x modified electrodes, as compared to 40% on SMF. The selectivity to CO_2 followed the same trend with the highest selectivity of ~30% for MnO_x/SMF. As MnO_x/SMF catalytic electrode showed better performance, further studies were focused on destruction of 250 ppm of toluene as a function of SIE varied between 160 and 1650 J/l by changing the voltage between 12.5 and 22.5 kV, and frequency in the range 200–350 Hz. Fig. 3a and b show the conversion and selectivity to CO_x and CO_2, respectively, on MnO_x/SMF electrode as a function of SIE (voltage and frequency). As seen from Fig. 3a, increasing the frequency at constant voltage increases toluene conversion. For example, at 12.5 kV and 200 Hz, toluene conversion was 65%, which increased to 80% at 300 Hz. In a similar manner, at any voltage, increasing the frequency leads to higher conversion. However, it is worth mentioning that increasing frequency increases SIE. Interesting observation is that at any frequency, conversion >90% was achieved with voltage higher than 17.5 kV. At 200 Hz, ~100% conversion of toluene was achieved at ~300 J/l (22.5 kV), whereas a high SIE of 450 and 700 J/l were required to achieve the same result at 300 and 350 Hz, respectively. These results suggest that at low voltage and high frequency, conditions are close to the ignition threshold, where the discharge may not be uniform throughout the discharge volume [17].

The selectivity to gaseous products (CO and CO_2) formed in the above reaction is given Fig. 3b. As no other hydrocarbon except toluene was detected at the outlet, S_{CO_x} also represents the carbon balance. Hence, the selectivity of solid deposits can be estimated as $(1 - S_{CO_x})\%$. As seen from Fig. 3b, increasing both voltage and frequency leads to higher selectivity to CO_x. However, better results were achieved at 200 Hz as ~100% selectivity to gaseous products was achieved at ~300 J/l (22.5 kV). With increasing frequency to 300 Hz, SIE of 700 J/l (20 kV and 300 Hz) was required to destroy the toluene to CO_x without observing carbon-based deposits in the DBD reactor.

Fig. 3b also represents the CO_2 selectivity for MnO_x/SMF electrode, which follows the same trend as the conversion and selectivity to CO_x (Fig. 3a and b). When SIE was varied in the range 160–295 J/l (i.e. frequency 200 Hz), the maximum selectivity to CO_2 was around 65% at 295 J/l. With increasing frequency to 350 Hz, CO_2 selectivity of ~80% was achieved at 17.5 kV and corresponds to SIE 740 J/l. It is worth mention-

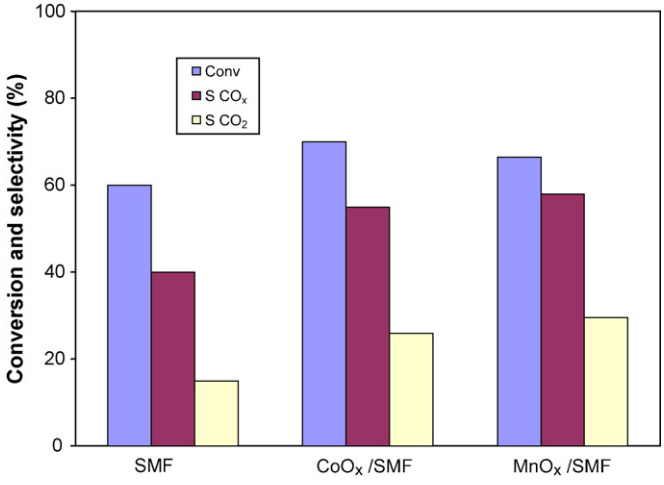

Fig. 2. Activity of the metal oxide modified SMF catalytic electrodes during the destruction of 250 ppm of toluene at 160 J/l (12.5 kV and 200 Hz).

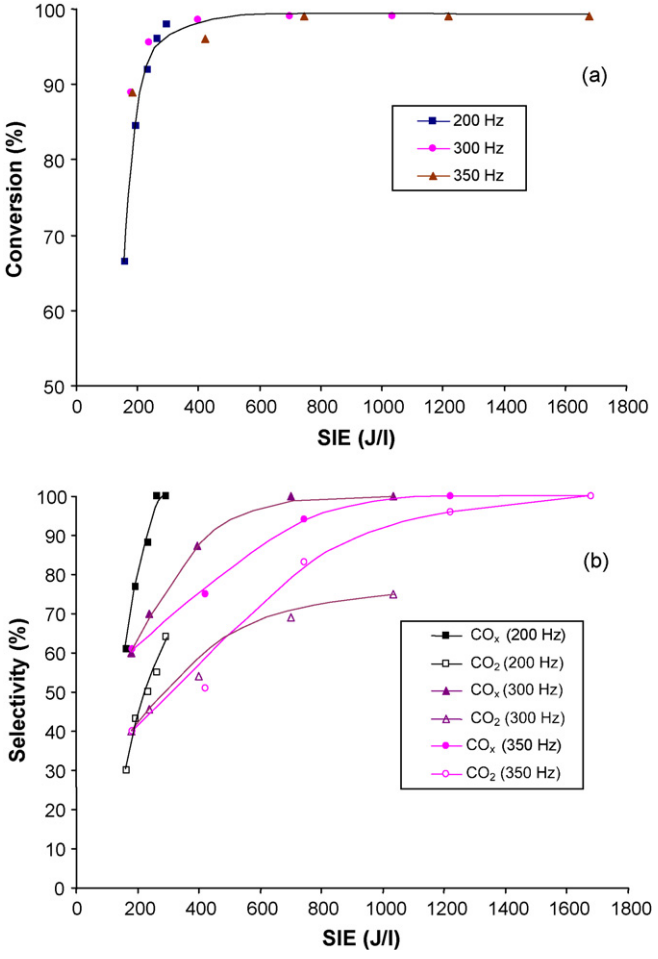

Fig. 3. Activity of the MnO_x/SMF catalytic electrode during the abatement of 250 ppm of toluene as a function of SIE on (a) conversion and (b) selectivity to CO_x and CO_2.

ing that at the same SIE, conversion and selectivity to CO_x was more than 90%. With further increasing voltage, CO_2 selectivity also increases to ~100% at 22.5 kV that corresponds to SIE of 1650 J/l. However, maintaining a SIE of 1650 J/l is not economically feasible since it exceeds an equivalent energy for heating the gas stream up to 700 °C.

3.3. Catalytic non-thermal plasma reactor for abatement of isopropanol

Alcohols are commonly used solvents in electronic industry. Isopropanol (IPA) is one of the solvents used for cleaning electronic chips, the printed circuit boards and LCD monitors. IPA from industrial effluent can be recovered by adsorption into water using wet scrubbers followed by distillation or pervaporation. Thermal oxidation of alcohols needs a high temperature in the range 600–700 °C, whereas, thermocatalytic oxidation takes place in the temperature range 250–400 °C [18]. However, these techniques are not suitable for the abatement of dilute alcohols. The NTP technique has already been tested for the destruction of IPA, however, formation of acetone as a stable secondary product was observed. Abatement of acetone demands a high energy (~1000 J/l), which is not energetically favorable [19,20]. During the present study, oxidation of 250 ppm of IPA over catalytic SMF electrodes has been carried out. Like-wise in the case of toluene, at a constant frequency of 200 Hz, metal oxide supported SMF electrodes showed better activity compared to SMF unmodified electrode. With the SMF electrode, the IPA conversion reaches ~100% only at 22.5 kV (295 J/l), whereas, with Co and Mn oxides supported SMF electrodes, it was achieved at 265 and 235 J/l, respectively.

Since MnO_x/SMF showed better activity during the oxidation of IPA, total oxidation of 250 ppm of IPA was carried out as a function of SIE varied in the range 160–760 J/l by changing the voltage and frequency in the range 12.5–22.5 kV and 200–275 Hz, respectively. As seen from Fig. 4a, the IPA conversion increases with the increasing applied voltage and frequency. At 200 Hz, ~100% conversion was achieved at SIE > 235 J/l (17.5 kV). However, with increasing frequency to 250 and 275 Hz, slightly higher SIE was required to attain ~100% conversion. Fig. 4b shows the selectivity to gaseous products formed in the above reaction. Increasing both voltage and frequency lead to higher selectivity to CO_x. At any frequency, nearly 100% selectivity to CO_x (with out solid deposit) was achieved at voltage higher 17.5 kV. The selectivity to CO_2 also followed the same trend. When SIE was varied in the range 160–295 J/l, maximum of 75% selectivity to CO_2 was achieved at 295 J/l (200 Hz, 22.5 kV) with ~25% selectivity to CO. With further increasing SIE to 500 J/l (22.5 kV and 250 Hz), the CO_2 selectivity reaches ~85%. Close to 100% CO_2 selectivity (no CO and carbon deposit) was achieved at 760 J/l (22.5 kV and 275 Hz).

3.4. Catalytic non-thermal plasma reactor for abatement of trichloroethylene

Chlorinated organic compounds especially trichloroethylene (TCE) is an effective cleaning agent for hydrophobic contaminants [1]. Catalytic and photocatalytic methods for the abatement of TCE produce by-products like phosgene and other toxic compounds. The NTP combined with MnO_x catalyst was observed to improve the efficiency of NTP reactor towards total oxidation [21]. During the present study, abatement of diluted TCE (250 ppm) was carried out with DBD reactor with catalytic SMF, CoO_x/SMF, and MnO_x/SMF electrodes.

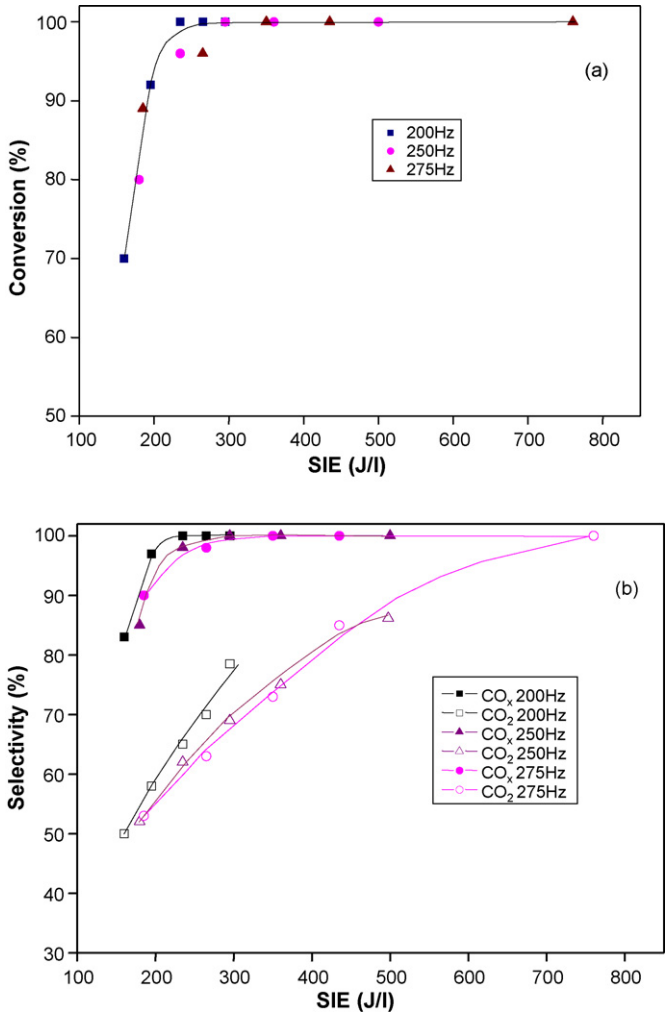

Fig. 4. Activity of the MnO_x/SMF catalytic electrode during the abatement of 250 ppm of isopropanol as a function of SIE on (a) conversion and (b) selectivity to CO_x and CO_2.

Fig. 5 represents the selectivity profile of MnO_x/SMF electrode as a function of SIE varied in the range 115–1200 J/l by varying the voltage (12.5–22.5 kV) and frequency (200–350 Hz) at a flow rate of 700 ml/min (STP). For all SIE, conversion ~100% was achieved except at 115 J/l (12.5 kV and 200 Hz), where conversion was ~90%. However, S_{CO_x} was not 100% even at 1200 J/l (22.5 kV and 350 Hz). This indicates the formation of various products as reported in the literature, but they were not identified during the present study [22]. The selectivity to CO_2 was only ~50% at 1200 J/l. In order to improve the performance of DBD reactor during the destruction of TCE, further studies were focused on decreasing the discharge gap and modification of the SMF electrode with a photocatalyst TiO_2.

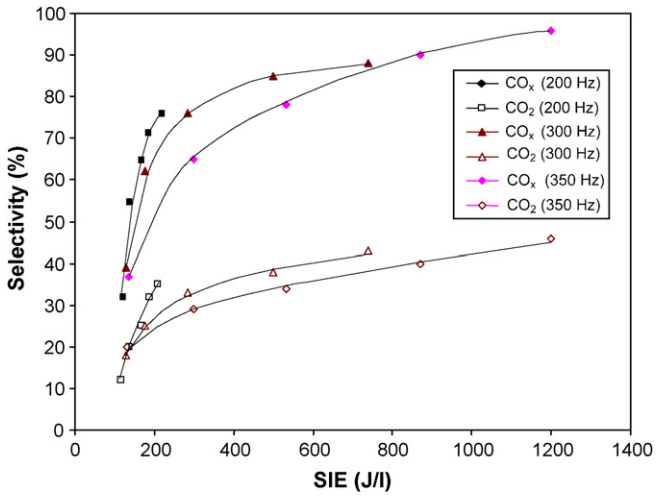

Fig. 5. Activity of the MnO_x/SMF catalytic electrode during the abatement of 250 ppm of tricholoroethylene as a function of SIE on selectivity to CO_x and CO_2.

Non-thermal plasma in air produces ultra-violet (UV) light, which comes from the excited nitrogen molecules. Attempts were done combining NTP with a photocatalyst TiO_2 for the destruction of VOCs [23,23]. However, the results indicate that the contribution of photocatalysis induced by UV light from plasma was <5%. In addition, the improvement in the activity was attributed only due to surface activation of TiO_2 by discharge plasma [23,24]. Nevertheless, the position of the photocatalyst should be optimized to utilize the UV light emitted by NTP. Plasma photocatalytic destruction of TEC was carried out using the novel DBD reactor with SMF electrode modified by TiO_2 and TiO_2/MnO_x in the SIE range 115–500 J/l (12.5–22.5 kV, 200 Hz) with a discharge gap of 1.25 mm. Typical results indicate that ~100% conversion of TCE throughout the range of SIE studied with SMF, CoO_x/SMF, MnO_x/SMF, TiO_2/SMF and TiO_2/MnO_x/SMF electrodes. At SIE 500 J/l (22.5 kV and 200 Hz) CO_x selectivity remains nearly the same (~90%) on all the above-mentioned catalytic electrodes. However, the selectivity to CO_2 was improved up to 70% with TiO_2/MnO_x/SMF from 15% on SMF. The selectivity to CO_2 follows the order TiO_2/MnO_x/SMF (70%) > MnO_x/SMF (58%) > CoO_x/SMF (50%) > TiO_2/SMF (30%) > SMF (15%). Further studies like characterization of the emission spectrum, influence of frequency on the selectivity to products and optimization of reaction conditions are in progress.

The regeneration of the catalytic electrodes was done by stopping the VOC flow and increasing the voltage to 25 kV until no CO_x was formed. The regenerated catalytic electrodes retained the original activity indicating the catalytic electrodes can be regenerated and used.

3.5. Formation of ozone

Ozone is an oxidizing species formed in NTP by the ionization of oxygen molecules [4,6,7,9–12]. During NTP catalytic abatement of VOCs, besides the direct reaction of ozone with VOCs, its catalytic decomposition leading to formation of atomic oxygen is a major reaction pathway [10]. Since ozone is a long-lived species, for both *in-plasma* and *post-plasma* catalytic reactors, it plays an important role during the oxidation of VOCs. However, the atomic oxygen formed due to *in situ* decomposition of ozone interacts with VOCs only when catalyst placed in discharge zone. During the present study, for 3.5 mm discharge gap, in the absence of VOC, increasing SIE increases ozone formation reaching a maximum of 1100 ppm at 200 J/l. Further increase of the SIE decreases ozone concentration and reaches zero above 295 J/l. Since the outlet gas temperature was <35 °C, thermal decomposition of ozone can be neglected. Hence, the decrease in the ozone concentration with increasing SIE may be due to the formation of other reactive species (nitrogen oxides) that can destroy ozone [13]. It is also interesting to note that on SMF electrode, at 200 J/l, the presence of VOC (toluene) decreased ozone formation to 800 ppm, which further decreased to 500 ppm with MnO_x/SMF. As observed from the data presented above, the best performance of the plasma reactor was achieved with catalytic MnO_x/SMF electrode, which shifted the product distribution towards total oxidation, whereas conversion remains nearly the same on all the catalysts. These results suggest that the better performance of MnO_x/SMF electrode might be due to the formation of atomic oxygen by *in situ* decomposition of ozone [25].

4. Discussion

The combination of NTP and heterogeneous catalyst allows an efficient removal of VOCs. The present DBD reactor configuration is beneficial over the reported designs. The specific advantages of using catalytic MnO_x (CoO_x)/SMF electrodes can be seen from two points: a high CO_2 selectivity at low input energy and minimization of solid deposit. With catalytic MnO_x/SMF electrode at low input energy, a significant increase in the conversion and selectivity to total oxidation products was achieved. With in-plasma catalytic reactor, synergy was due to the utilization of the short-lived oxidizing species like oxygen radical anion (O_n^{-1}) and electronically activated (O_2^*). With the DBD reactor containing catalytic electrode, it is possible to overcome the limitations of in-plasma catalytic reactor avoiding the carbon deposit. The better performance of MnO_x/SMF compared to other electrodes was demonstrated and attributed to atomic oxygen formed by *in situ* decomposition of ozone [25]. The surface atomic oxygen interacts with partially oxidized organics leading to a high selectivity towards CO_2 formation. Close to 100% selectivity to CO_x and CO_2 was achieved by varying voltage and/or frequency.

5. Conclusions

(1) A novel concept of utilizing a metallic catalyst made of sintered metal fiber (SMF) as the inner electrode has been used to design a dielectric barrier discharge (DBD) reactor.
(2) The SMF electrode was modified with transition metal oxides and tested for the destruction of dilute volatile organic compounds (VOCs) of different nature like toluene, isopropanol and trichloroethylene. Close to 100% destruc-

tion of 250 ppm of VOCs was achieved at specific input energy $\leq$250 J/l.

(3) The MnO_x/SMF showed the best performance for the complete oxidation of toluene and isopropanol to CO_2 and H_2O at reasonable specific input energy.

(4) During the destruction of 250 ppm of trichloroethylene, modification of SMF with a photocatalyst (TiO_2) improved CO_2 selectivity up to $\sim$70% with TiO_2/MnO_x/SMF electrode against 15% on SMF.

Acknowledgements

The authors acknowledge the Swiss National Science Foundation ("SCOPES" program) and the Swiss Commission of Technology and Innovation (CTI, Bern) for the financial support.

References

[1] K. Urashima, J.S. Chang, IEEE Trans. Ind. Appl. 7 (2000) 602.
[2] K.P. Francke, H. Miessner, R. Rudolph, Plasma Chem. Plasma Process. 20 (2000) 393.
[3] T. Oda, J. Electrostat. 57 (2003) 293.
[4] U. Kogelschatz, Plasma Chem. Plasma Process. 23 (2003) 1.
[5] F. Holzer, U. Roland, F.D. Kopinke, Appl. Catal. B: Environ. 38 (2002) 163.
[6] M. Magureanu, N.B. Mandache, P. Eloy, E.M. Gaigneaux, V.I. Parvulescu, Appl. Catal. B: Environ. 61 (2005) 13.
[7] B. Penetratnte, M.C. Hsiao, J.N. Bardsley, B.T. Merrit, G.E. Vogtlin, A. Kuthi, C.P. Burkhart, J.R. Bayless, Plasma Sources Sci. Technol. 6 (1997) 251.
[8] Y.H. Song, S.J. Kim, K. Choi, T. Yamamoto, J. Electrostat. 55 (2002) 189.
[9] U. Roland, F. Holzer, F.D. Kopinke, Appl. Catal. B: Environ. 58 (2005) 217.
[10] U. Roland, F. Holzer, F.D. Kopinke, Appl. Catal. B: Environ. 58 (2005) 227.
[11] U. Roland, F. Holzer, F.D. Kopinke, Catal. Today 73 (2002) 315.
[12] S. Futamura, A. Zhang, G. Prieto, T. Yamamoto, IEEE Trans. Ind. Appl. 34 (1998) 967.
[13] H.H. Kim, S.M. Oh, A. Ogata, S. Futamura, Appl. Catal. B: Environ. 56 (2005) 213.
[14] A. Ogata, K. Mizuno, S. Kushiyama, T. Yamamoto, Plasma Chem. Plasma Process. 19 (1999) 383.
[15] C. Ayrault, J. Barrault, N. Blin-Simiand, F. Jorand, S. Pasquiers, A. Rousseau, J.M. Tatibouet, Catal. Today 89 (2004) 75.
[16] Ch. Subrahmanyam, M. Magureanu, A. Renken, L. Kiwi-Minsker, Appl. Catal. B: Environ. 65 (2006) 150.
[17] Ch. Subrahmanyam, A. Renken, L. Kiwi-Minsker, Appl. Catal. B: Environ. 65 (2006) 157.
[18] J.M. Gallardo-Amores, T. Armaroli, G. Ramis, E. Finocchio, G. Busca, Appl. Catal. B: Environ. 22 (1999) 249.
[19] Z. Falkenstein, J. Adv. Oxid. Technol. 2 (1997) 223.
[20] J.J. Coogan, Technologie Transfer # 97023244A-ENG, LANL, February 1997.
[21] T. Oda, T. Takahashi, K. Yamaji, IEEE Trans. Ind. Appl. 40 (2004) 1249.
[22] S. Futuamura, A.H. Zhang, T. Yamamoto, J. Electrostat. 42 (1997) 51.
[23] T. Sano, N. Negishi, E. Sakai, S. Matsuzawa, J. Mol. Catal. A: Chem. 245 (2006) 235.
[24] A. Ogata, H.H. Kim, S. Futamura, S. Kushiyama, K. Mizuno, Appl. Catal. B: Environ. 53 (2004) 175.
[25] S. Futamura, H. Einaga, H. Kabashima, L.Y. Hwan, Catal. Today 89 (2004) 89.